RGNZ/MGPB

An Innovative Approach to Optimize the Comminution Circuit of Micronized Powder Production Plant

Rudarsko-geološko-naftni zbornik
(The Mining-Geology-Petroleum Engineering Bulletin)
DOI: 10.17794/rgn.2026.1.9

Original scientific paper

Alireza Ghorbanifar[1] ✉, Marzieh Hosseini Nasab[2]* ✉, Javad Alibabaii[3] ✉, Mohammad Noaparast[3] ✉

[1] *Department of Mining Engineering, Tehran Science and Research branch, Islamic Azad University, Tehran, Iran.*

[2] *Department of Mining Engineering, Faculty of Engineering, University of Sistan and Baluchestan, Zahedan, Iran.*

[3] *School of Mining Engineering, College of Engineering, University of Tehran, 1417466191, Tehran, Iran.*

Abstract

This research was conducted to investigate and optimize the comminution circuit of the Arak Company in which bentonite micronized powder is produced. The criterion for evaluating was the optimal performance of grinding systems and the efficiency of the devices, and simultaneous optimization was considered in feed and product sizes, capacity, and energy. In addition to the Bond formula, Morrell and Austin relations, as an innovative approach, have also been employed to study the different parameters such as rotation speed and mill filling percent. In this unit, the main grinding operation is performed by a tube ball mill that is located in a closed circuit with two air separators. The size of the final product is finer than 75 microns, and 48 kilowatt-hours of energy are consumed to produce one ton of bentonite. About 59% of the total plant energy consumption was related to the grinding circuit of tube mill. The size of the tube mill feed was 3500 microns (d_{80}), the percentage of charge and accumulation were 21 and 14% respectively, the average diameter of the steel balls was 60 mm and the relative rotation speed of the mill was 79%. The results showed that the efficiency of the grinding circuit is poor, and it was merely about 30%. By increasing the percentage of charge of the tube mill from 21 to 70%, increasing the size of the mill feed by 7000 microns, using balls with diameter of <40 mm, and reducing the relative rotation to 60%, the efficiency of the grinding circuit can be increased by 50%. It would be noted that about 16% of the coarse particles in tube mill's product are agglomerated pieces. Therefore, reducing this phenomenon will have a direct effect on the reducing energy consumption and increasing grinding efficiency, as well.

Keywords:

micronized powder; efficiency; tube mill; bentonite; Morrell and Austin relations

1. Introduction

Bentonite is one of the important non-metallic minerals whose micronized powder is widely used in industry (**Kutlić et al., 2012; Vetyugov and Matveeva, 2024**). Bentonite refers to clay soil that is essentially composed of montmorillonite (**Kutlić et al., 2012; Ngcobo et al., 2022**). Its color is often white, pale green, pale blue (fresh surface) to cream (weathered surface), gradually tending to yellow, red and brown (**Kutlić et al., 2012**). Feldspar, biotite and quartz minerals are usually found together with bentonite (**Grim and Guven, 2011**). Bentonites have exchangeable ions of sodium, calcium and magnesium (**Kutlić et al., 2012**), and after zeolites, they show the highest ion exchange capacity among minerals (**Bentonite, 2005; Kutlić et al., 2012**).

Each of the various applications of bentonite requires specific properties, which are summarized below. For drilling mud, mud recovery (the amount of bentonite mud with an apparent viscosity of 15 centipoise obtained from one ton of clay), gel strength (the difference in weight recovery over a 10-minute period after mixing), wall-forming property (the amount of water loss through a filter paper when a bentonite pulp with an apparent viscosity of 15 centipoise is subjected to 100 psi), and particle size (97.5% finer than 75 microns) are among the important properties (**Kutlić et al., 2012**).

In the case of casting, the chemical composition of bentonite is usually 92% montmorillonite, 3% quartz, and 5% feldspar, 6-12% moisture, pH 8.3, green compressive strength of 656 kPa, and a particle size of 65-95% finer than 75 microns. In pelletizing, particle size is a very significant issue, typically 70-90% finer than 45 microns, with moisture content of up to 10% being appropriate (**Bentonite, 2005; Stojiljković and Stojiljković, 2017**). In the case of using bentonite to make a floor or wall impermeable, clay with 80-90% bentonite with particle size of 840 to 300 microns is required (**Kutlić et al., 2012**). The use of bentonite as an adsorbent for removing heavy metals from wastewater also

* Corresponding author: Marzieh Hosseini Nasab
e-mail address: hosseininasab@eng.usb.ac.ir

Received: 3 July 2025. Accepted: 5 September 2025.
Available online: 2 January 2026

depends on pH, contact time, temperature, and amount of adsorbent used (**Alsaeed et al., 2022; Rockson-Itiveh et al., 2023; Lamrani et al., 2025**). Bentonite clay is known for its exceptional water absorption and swelling properties, primarily due to its composition of the clay mineral montmorillonite. This clay can absorb significant amounts of water, expanding its volume considerably, and also exhibits high cation exchange capacity and low permeability. Specific gravity: 2·8 ± 0·03, Room water content: 6–8%, Montmorillonite content: 53%, Main accessory minerals: quartz, feldspar, plagioclase, calcite, Content of particles of size<5 μm: 73%, Liquid limit: 505%; Plastic limit: 45%, and Cation exchange capacity: 71·9 meq/100 g are necessary for water absorption and swelling properties (**Wang et al., 2024**).

Due to the abundance of bentonite in nature and the extensiveness of its reserves in most countries of the world, high-quality reserves are usually extracted. As a result, bentonite processing is in most cases limited to crushing and grinding, which only includes drying and breakage, using various mills. Therefore, bentonite must be of good initial quality, because no separation operations are performed on it (**Kutlić et al., 2012**). The production of bentonite powder is often used by steelmaking industries and drilling companies and is purchased in bulk. The characteristics of the product desired by the two steel and drilling companies are given in **Table 1**.

Table 1. Product characteristics

Employer	Steel Company - Drilling Company
Size distribution	Maximum 3% remaining on 45 microns sieve
Montmorillonite content by XRD analysis	92%
Mud recovery	22 (one ton of bentonite powder has the ability to produce 22 cubic meters of drilling mud with a viscosity of 15 centipoise)
Water absorption	600%
Moisture	8-12%

In general, comminution including crushing and grinding system is the most important and fundamental stage of processing various ores, because it is at the beginning of the mineral processing stages and accounts for the highest fixed and operating/current costs (50-70% of energy consumption) (**Bogdanov et al., 2022**; **Li, 2024**). Therefore, optimizing energy consumption in comminution systems will have a great impact on reducing energy consumption in all mineral processing plants (**Khurmamatov and Mukhamedbaev, 2023**). Considering the above, implementing optimization systems in mining units and related industries is inevitable (**Asa'd and Levesque, 2024; Elbendari and Ibrahim, 2025; Khan et al., 2025; Yıldırım et al., 2025**).

The main purpose of this research is to study and investigate the performance of the devices in the Arak micronized powder production plant and, based on the results, to provide necessary optimization solutions, with an innovation in employing Austin and Morrell equations.

1.1. Research Objectives

- The process of producing bentonite powder is usually carried out using a ball mill, and in this research, the use of a tube mill instead of a ball mill was investigated and an attempt was made to optimize it.
- One of the properties of bentonite, like other clays, is its re-adhesion after the micronized process. This issue was observed and investigated in this research.
- The comminution of material, and classification in air classifier was evident in this research and was addressed.
- Providing a scientific and operational method for examining the performance of the production line.
- Providing solutions and suggestions for further comparative studies.

1.2. Description of the production process

First, the ore is supplied from the mines with initial sizes up to 30 cm and is deposited, and is reported for further size reduction process. Then, these materials are conducted into a jaw crusher with an opening of 15 cm. Of course, particles larger than 15 cm are crushed on site. It should be noted that due to the smaller dimensions of bentonite than the outlet opening of the jaw crusher, they do not usually tolerate the breakage, and merely pass the jaw crusher with no changes to their size. However, jaw crusher product is then fed into the dryer, by a conveyor belt until their moisture content reaches the permissible limit (**Kutlić et al., 2012**). Then, the materials enter the hammer mill and, after being crushed to a size finer than 12 mm, are transferred to the material storage bin, by a bucket elevator. From the bin, they are directed to a tube mill by a feeder to be micronized into particles finer than 75 microns. The milled product is forwarded to two air classifiers, and after separation, the coarse particles are transported by screws to the beginning of the mill inlet (circulating load), and the fine particles (final product) are directed to the product bunker.

1.2.1. Tube mill

In most micronized powder plants, a jaw crusher, hammer mill, and ball or roller mills are normally used, respectively. This plant has two independent micronized powder production lines. In this production unit, the materials crushed by the hammer mill enter a 15-ton bin and from there, they enter to the tube mill along with the

Table 2. Specifications of the tube mill

Type of mill	Tube mill (ball-ball)
Discharge type	full screen
Internal mill diameter	1.54 m
Internal length of the mill	5.2 m
Internal volume	9.3 m^3
Length of each chamber	2.6 m
Middle screen opening	5 mm
End screen opening	3 mm
Grinding load	steel balls in sizes 85, 55 and 40 mm
Specific mass of balls	7.5 g/cm^3
Liner type	Steel type
Driven force type	electric motor and gearbox
Nominal motor power	250 kW
Rotation speed	26 rpm

circulating load. The amount of materials entering the tube mill from the bin is adjusted manually by the valve. One of the characteristics of tube mills is the presence of a diaphragm between the two chambers or compartments, which performs the particles classification. The diaphragm separates the two chambers of the mill from each other, and prevents the passage of coarse particles to the next one. The diaphragms could control the material level inside the chambers and therefore prevent dead space in the breakage areas, by using the material flow mechanism.

This tube mill consists of two chambers with a length of 2.6 meters. The materials in the first chamber are ground due to the presence of a middle screen with an opening of 5 to 15 millimeters and enter the second chamber for the grinding and micronized stage. The opening of the final screen is 3 mm. The materials were ground in the first chamber pass through the screen by the air flow and the pressure of the load inside the mill. At the end of the mill, a fan with a cyclone is installed to accelerate the movement of the materials to the mill and the dust and particles resulting from this process are collected and directed to the cyclones as well. The fan motor rotation speed is 1300 rpm and at the end of each 8-hour work shift and/or for every 20 tons of products, about 400 kg of fine particles are collected which are transferred to the classifier inlet again. Considering that the main burden of the grinding operation is mostly related to the tube mill and the highest energy consumption is accordingly by this device, the focus of this research is on examining the tube mill grinding circuit. The specifications of the tube mill are given in **Table 2**.

1.3. Mechanism and relevant parameters in comminution circuit

One of the most important and fundamental units of mineral processing is comminution system which consists of crushing and grinding stages (**Matsanga et al., 2023; Upadhyay, 2025**). The goals of comminution include releasing valuable minerals, producing particles with specific dimensions and shapes, and increasing the specific surface area for various reactions (**Khan et al., 2025; Yıldırım et al., 2025**). With the optimal performance of the comminution circuit, in addition to significant energy saving, the optimization of subsequent processing stages is also facilitated (**Chimwani and Bwalya, 2021; Shields et al., 2024; Elbendari and Ibrahim, 2025; Wan et al., 2024**).

In order to optimize each size reduction line, four main criteria (feed and product sizes, capacity, and energy) are needed to be in their optimal state (**Lowrison, 1974; Prasher, 1987; Mular et al., 2002**). The relationships and interactions between these four criteria are expressed by Bond's equation. Bond's equation is the most common approach to estimate the required energy by crushers and mills. Of course, this method also has some shortcomings, for example, the critical speed, the filling amount and the particles residence time in the mill, and the portion percentage of feed particles which are finer than the product are not considered. If the kinetics and the mode of breakage, as well as the time of grinding are known, in fact, all aspects of grinding are accordingly considered. The kinetics of grinding and the mode of breakage are called the selection and breakage functions, respectively, and the grinding time is also described by the residence time distribution. The breakage function parameter does not change with variation of the grinding conditions, and therefore is not involved in the optimization criteria. However, the selection function depends on the grinding conditions such as mill diameter, volume and diameter of balls used, mill rotation speed and the filling percentage the mill by powder (**Bond, 1961a; Bond, 1961b; Lowrison, 1974; Austin et al., 1984; Prasher, 1987; Mular et al., 2002**). Therefore, in addition to the Bond relation, which is based on the main parameters of the comminution circuit such as the feed and product sizes, the formulas and relations of Morrell and Austin have also been employed which is an innovation in order to calculate and investigate the effect of secondary parameters such as the rotation speed and the degree of filling of the mill (**Morrell, 2019b; Austin, 1990; Golpayegani and Rezai, 2022**).

In this research, after presenting the circuit grinding mechanisms, the effective parameters in optimizing the grinding circuit were investigated, for which the applied procedure is shown in **Figure 1**.

1.3.1. Ball trajectory tracking with image processing system

Usually, optimization and design of milling circuits is based on laboratory and semi-industrial studies. One of the methods of validating the experiments is tracking the ball trajectory and monitoring the mill power draw on a

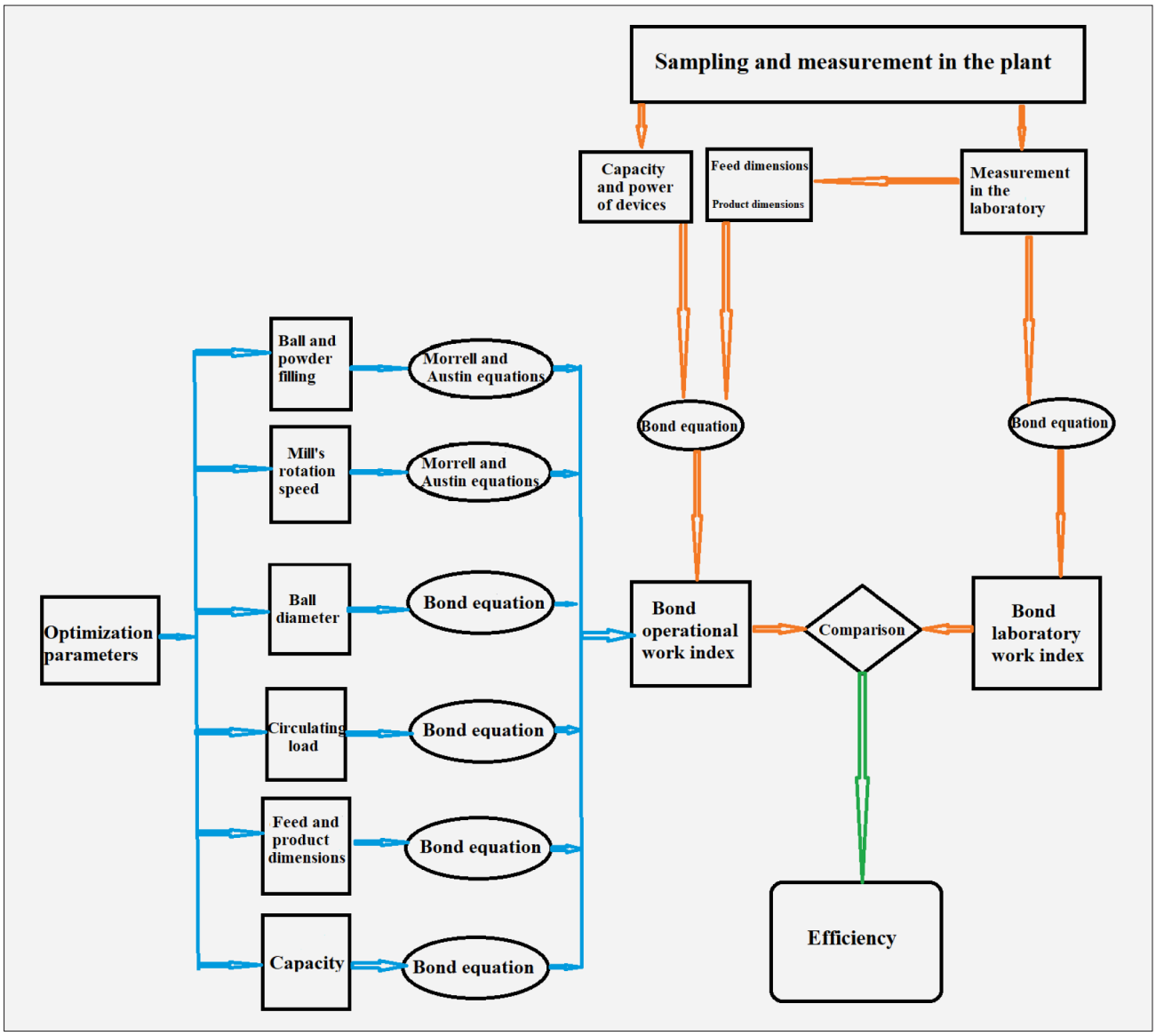

Figure 1. Summary of operations for calculating efficiency and optimizing the grinding line

laboratory scale (**Li et al., 2022**). The balls trajectory tracking and velocity monitoring are also performed with an image processing system (**Maleki-Moghaddam et al., 2013; Makgoale, 2019; Bian et al., 2017**). The results of a series of image processing experiments using a camera to record the motion of the charge under different operating conditions with a high-intensity light source and a laboratory-scale ball mill, with a constant rotation speed of 52.75% of the critical speed (37.31 rpm) and varying the liner type and percentage of charge (0.5, 20, 40 and 60) and measuring the shoulder and heel angle parameters, which indicate the following (**Mori et al., 2004**):

- The liner type has a significant effect on the charge profile and the improvement of the cascade motion is a function of the load level in the mill.
- Increasing the load level from 20-40% reduces the cascade. The velocity of balls is balanced, the distance between the load surface and the heel is reduced and the ball impact velocity at the heel is also reduced. Therefore, its effect also reduces the kinetics energy resulting from the impact of the balls, accordingly.
- As shown in **Figure 2**, increasing the load level by 60% reduces the cascade effect. The type of liner has a significant effect and under these operating conditions the mill product becomes finer.

1.3.2. Bond Work Index

The relationship between the ore breaking ability and the energy required for the grinding device is expressed by Bond's equation. The energy required for the size of ore from the feed size $d_{80,\,F}$ to the product size $d_{80,\,P}$ is given by Bond's equation, which is defined in **Equation 1** with P_0 in terms of (kWh/t) (**Bond, 1961a; Bond, 1961b**).

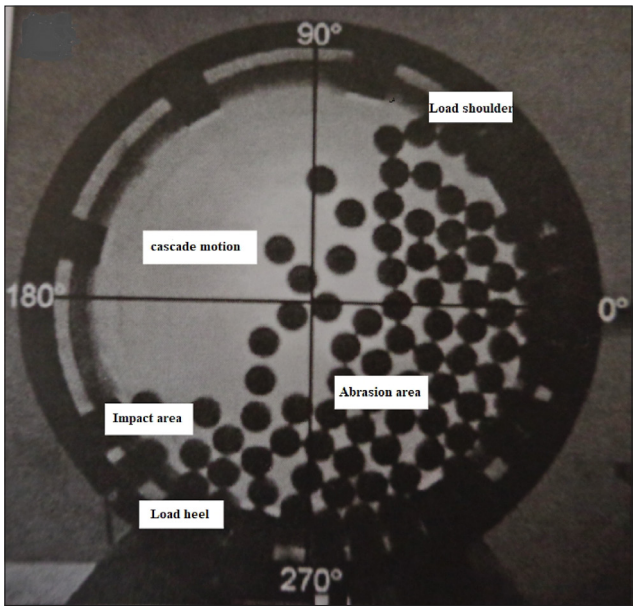

Figure 2. Charge movement profile and mechanism in mill at 60% occupancy (**Fuerstenau and Han, 2003**)

$$P_0 = 10\, w_i \left[\frac{1}{(d_{80,P})^{0.5}} - \frac{1}{(d_{80,F})^{0.5}}\right] \quad (1)$$

The work index (w_i) is defined as the reference energy required to reduce hypothetically one short ton (907 kg) of material from very large size (theoretically infinite/extreme size) to reach to product size of 100 microns. This index is normally used to determine the energy required for equipment design, such as crushers and some tumbling grinding mills (rod and ball mills), optimization of an active circuit to reduce energy consumption and increase efficiency. The control of the energy required for the process and the determination and selection of mills are also evaluated with this parameter. The larger this index, the more resistant the ore is to be ground, 7-10 kWh/t for soft ores, 10-15 kWh/t for medium to hard ores, and up to 25 kWh/t for relatively very hard materials as well (**Morrell, 2019b**).

In **Equation 1**, feed and product d_{80} are in microns and the sizes are conventionally the screen sizes which have 80% of the particles passing through it. The ores work index value is determined by a standard laboratory method. Based on the definition of Bond, there are standard studies to measure the value of the Bond work index to accurately obtain the power required for a wet ball mill. In this method, an overflow type ball mill with 2.44 m diameter has been specified, operating in a closed circuit with a classifier at 250% of circulating load. The ore used is of very coarse size which has to be reached 80% finer than 100 microns, and the amount of energy consumed will accordingly be equal to the work index of the used ore being tested. Given the difficulty of this method for determining the work index, the standard Bond method was experimentally defined (**Bond, 1961a; Bond, 1961b**). It should be noted that the work index of a specific ore, as measured using the standard laboratory method, is usually not directly comparable to its grinding conditions in an industrial environment and some relevant correction factors must be applied. In addition, to evaluate a ball or rod mill power that is to grind W t/h of material, it is necessary to calculate the power required for grinding from **Equation 2** (**Lowrison, 1974**):

$$P = P_0 \times W \quad (2)$$

1.3.2.1. Bond Laboratory and Operational Work Index

In order to determine the laboratory work index, the Bond standard ball mill method is usually used. In this test, the grinding and classification operations are carried out in a dry manner to achieve equilibrium conditions. The dimensions of the required mill are 305×305 mm (diameter × length) rotating at a speed of 70 rpm. Its balls load is 285 steel balls weighing 22.311 kg. Using the Bond formula (**Equation 3**), the laboratory work index is obtained using the Bond standard ball mill procedure (**Bond, 1961a; Bond, 1961b**).

$$w_{i,lab} = \frac{44.5}{\left[\left(P_1^{\,0.23}\right) \times \left(G_i^{\,0.82}\right)\right]} \times \left(\frac{10}{\sqrt{P_{80}}} - \frac{10}{\sqrt{F_{80}}}\right)^{-1} \quad (3)$$

Where w_i is the work index (kWh), F_{80} and P_{80} are the sizes which 80% of the feed and final product are finer, respectively. P_1 is the control screen (microns) and G_i is the weight of particles finer than the control screen in grams produced from one mill cycle (rotation).

The operational work index $w_{i(op)}$ is calculated by measuring the net power consumed by the mill in a given time interval to grind a given tonnage of mineral material and by substituting it into the bond formula (**Equations 1** and **2**), based on **Equation 4**.

$$w_{i(op)} = \frac{W}{\left[Q\left(\frac{11}{\sqrt{P_{80}}} - \frac{11}{\sqrt{F_{80}}}\right)\right]} \quad (4)$$

Where:

$w_{i(op)}$ – operating work index (kWh/t),
Q – mill input tonnage (t/h),
P_{80} – Mill product size (microns),
F_{80} – Mill feed size (microns),
W – net power (kW).

1.3.2.2. Energy consumption and efficiency

In general, the energy consumption in the mineral comminution line is very high and directly affects the consumption costs of the plant as well. Therefore, periodic monitoring of the operation and efficiency of the devices is accordingly inevitable (**Golpayegani and Rezai, 2022**). In order to determine the grinding effi-

Table 3. Efficiency classification based on the ratio of the bond work index (**Lowrison, 1974**)

Efficiency	$w_{i(lab)}/w_{i(opt)}$
Ideal	1
Good	0.9
Acceptable	0.7
Poor	Less than 0.7

ciency, based on **Table 3**, the ratio of the laboratory and operational work index is used (**Bond, 1961a; Bond, 1961b**).

Two types of mill inefficiency could happen within the grinding process: indirect and direct inefficiency (**Austin et al., 1984; Kelly and Spottiswood, 1989; Morrell, 2009**). Indirect inefficiency takes place when the mill can break ores efficiently, but energy is wasted in the overgrinding of materials which are fine enough, and consequently more fines are produced. This state is mostly observed when the circulating load is not adjusted. The second type is direct inefficiency, which occurs when the mill conditions cause poor breakage. The reasons for poor breakage could stem from overfilling of the load and powder inside the mill, and therefore the ball-powder-ball is weak because of the thick mass cushion. Another issue is underfilling of the load and powder inside mill, which causes energy to be used for ball-ball-liner action, and is not efficiently applied on particles (**Austin et al., 1984; Kelly and Spottiswood, 1989; Morrell, 2009**).

It is worth mentioning that one more type of inefficiency could happen, which is related to defects in the energy supply and transmission system (dynamo, shaft, gearbox, etc.), and this is not due to process conditions.

1.3.3. Morrell and Austin relationships

In order to predict the tensile strength of ball, autogenous (AG) and semi-autogenous (SAG) mills, valid equations and models have been presented by Morrell and Austin (**Austin, 1990; Morrell, 1993; Morrell, 2016; Morrell, 2019a; Morrell, 2019b; Golpayegani and Rezai, 2022**). These relations have been used to calculate the net power of the tube mill and to select the optimization parameters (**Equations 5, 6** and **7**) (**Morrison and Morrel, 1997; Morrell, 1996; Morrell, 2004**).

$$\text{Gross power} = \text{net draw power by load} + \text{power at no load} \quad (5)$$

$$P_t = KD_m^{2.5} L_e \rho_c \alpha \delta \quad (6)$$

$$P_e = 1.68 D_m^{2.5} [\varphi_c (0.667 L_d + L)]^{0.82} \quad (7)$$

Where:

P_t – Gross power (kWh),

P_e – No-load power (kWh),

D_m – Internal diameter of the mill (m),

L_e – Effective length of the mill, including the conical end (m),

ρ_c – Specific gravity of the total load of materials inside the mill (including the crushed load and pulp inside the mill),

K – Calibration constant that varies with the type of discharge (for mills with overflow discharge it is 7.98 and for mill with grate discharge it is 9.1),

L_d – Average length of the two conical ends and is calculated from half the difference between the central length of the mill and the length of its cylindrical section.

Austin also proposed the following relations for calculating α and δ (**Austin, 1990**):

$$\alpha = J_t(1 - 1.03J_t) \quad (8)$$

$$\delta = \varphi_c \left[1 - \left({}^{0.1}/_{2^{9-10\varphi_c}}\right)\right] \quad (9)$$

φ_c – Mill speed relative to critical speed,

J_t – Part of the mill occupied by the total load,

α – Factor related to the relative degree of filling,

δ – Factor related to the rotation speed.

1.3.4. Circulating Load

In many industries, the milled product must be finer than a certain size, but the presence of excess fines is also undesirable. The presence of less fines in product, results in a steeper size distribution curve, which means the product distribution would be a narrow size. Therefore, an important and general principle in grinding is to prevent excess fine production. It is therefore essential for materials that have been sufficiently fined are removed from the circuit quickly, in order to prevent the overgrinding of particles. In an open circuit where there is no size classification device (classifier) in the circuit, sufficiently fine particles move through the mill and become finer, while at the same time coarse particles are ground as well. The presence of a classifier or a closed circuit means that the mill operates at a higher flow rate (fresh feed plus circulating load), resulting in the particles having a shorter residence time. If the initial flow rate is Q t/h and the circulating load is T t/h, the whole feed of mill is Q+T. This flow rate, higher than Q, causes the material to exit the mill more quickly. Therefore, the fines are separated inside the classifier and the coarse particles return to the mill for further breakage. The final effect would be that the size distribution particles inside the mill would shift to the presence of coarser particles and the finer particles have a shorter residence time. Accordingly, less over-grinding of fine particles and reducing the amount of very fine particles production occurs. Therefore, circulating load in grinding circuits would play a key role in order to control the amount of fines production (**Wills, 1997**).

2. Materials and Methods

2.1. Evaluation of the comminution circuit

In this study, the comminution circuit of Arak bentonite Micronized Powder Company was evaluated. In order to evaluate the comminution circuit, it the current line should be reviewed and parameters which are effective in optimization should be calculated and compared with the initial design values (if any). To evaluate the current line, the following seven steps were considered:

- Sampling from different points of circuit;
- Measuring the input and output tonnage of different parts of the production line, the input load to the plant, the input and output of the mills and classifiers;
- Measuring the electric currency of each device from the electrical panel to calculate the power consumption;
- Running sieve analysis tests and determining the particle size, and also determining the laboratory bond index;
- Calculations related to energy consumption and determining the devices efficiencies;
- Material and energy balance of the comminution circuit;
- Calculations related to other parameters effective in optimization.

Table 4. Sampling location and amount

Row	Sampling location	Number of samples
1	Initial material Heap	1
2	Hammer mill outlet	four 5 kg samples
3	Tube mill outlet	four 3 kg samples
4	Coarse grain of classifier	four 3 kg samples
5	Fine grain of classifier	four 3 kg samples

2.2. Equipment used for testing

The equipment used in this research is divided into two parts:

- Required and handmade sieves for granulating the incoming load from the mine in the production unit;
- Standard laboratory equipment including:
  - ASTM standard laboratory sieves;
  - Digital scale with an accuracy of one hundredth of a gram;
  - Bond ball mill;
  - Sample divider.

2.3. Sampling

In order to control the operations in a mineral processing plant and adjust it, to achieve appropriate conditions, it is necessary to examine the load of different plant streams, in terms of quality and quantity. This requires having samples that represent the load of those streams. Sampling may be manual or automatic, and measurement of the desired parameters in each stream was carried out on the samples taken. It was obvious that the desired tests must also be carried out with sufficient accuracy, otherwise subsequent analyses would be disrupted (**Wills, 1997**).

According to **Table 4**, the minimum sample weight required from the initial load of the plant, and the hammer mill output was calculated as 3768 and 3 kg, respectively (based on Gy's equation), and in the implementation, the weight of the tested samples was considered close to the calculated weights. The results of the calculations to determine the minimum sample weight of the tube mill and classifier output (9, 21 and 0.05 g) were very low and not applicable. Therefore, by modelling and reviewing similar research studies (**Dehghani et al., 2016; Dehghan et al., 2008**), samples with an approximate weight of 350 and 90 g were supplied.

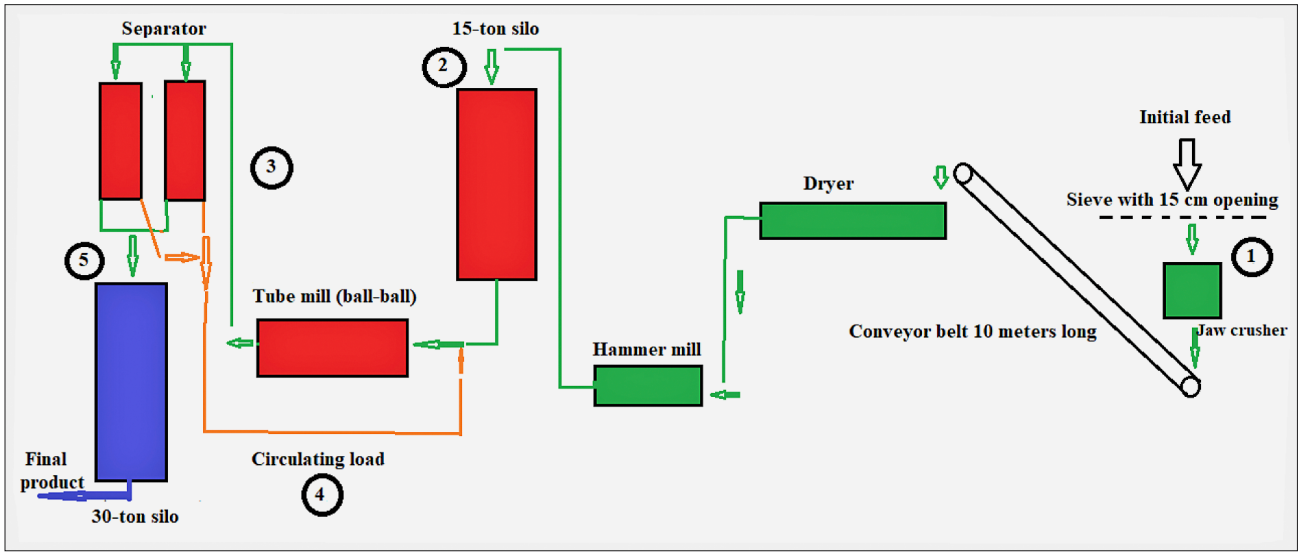

Figure 3. Flowsheet of the micronized powder production line, and sampling points

2.3.1. Sampling from the plant's feed (run-off-mine)

To supply from the plant's feed, 4 trucks were unloaded in a cone shape with about 72 tons. Using a large loader, a quarter of the load weighing approximately 18 tons was separated and placed in a cone, at another location, and from this load, another quarter weighing approximately 4 tons was transferred by a small loader as a representative sample. Initially, large pieces of mineral material with dimensions greater than 15 cm were crushed. After running a sieve analysis test, the particle size distribution was determined by sieves with openings of 10, 7.5, 4.5, 3.2, 2.5 and 1.1 cm, and a graph of cumulative percentage passing through the sieve was drawn to determine relevant d_{80}.

2.3.2. Sampling from the production line

Initially, flow rates were measured and samples were taken from different points of the plant, numbers 2 to 5 according to the flow sheet in **Figure 3**, twice per shift (at 4-hour intervals) over 2 consecutive days. Sampling was performed manually from the flanges of the connection pipes of the grinding circuit.

Table 5. Results of Sieve Analysis Tests

d_{80} plant's feed	73 mm
d_{80} hammer mill product	8.5 mm
d_{80} tube mill feed	3350 μm
d_{80} classifier feed	380 μm
d_{80} classifier coarse part (circulating load)	380 μm
d_{80} classifier fine part (product)	48 μm

Table 6. Electricity consumption and product tonnage at the Arak Company in two months

Time period	Electricity consumption (kWh)	Product tonnage	Energy required for one ton (kWh)
First month	21600	440	49
Second month	14500	305	47
Total	36100	745	48

3. Results and discussions

Based on sampling and sieve analysis tests, the results of the particle size distribution of each stage of comminution circuit were determined, including the plant input, from the hammer mill output, the tube mill input, the classifiers input, from circulating load, and finally from plant's output. A summary of the performed tests results which are required for further and subsequent calculations is given in **Table 5**.

Using the information in **Table 5** and assuming a control screen of 150 microns, the work index value was calculated, according to **Equation 3**, which is equal to 5.9 kWh/st, or 6.37 kWh/t by applying a coefficient of 1.1 (converting short to metric ton). According to the classification presented in the energy consumption and efficiency section, the calculated work index was lower than 7 kWh/t, and it therefore is classified as a very soft material.

3.1. Material and energy balance

Since most of the energy required for the comminution circuit is supplied by electrical energy, so by examining the average consumption in two months, and the tonnage of the product for each month, the average energy needed for bentonite breakage to a size of 75 microns was determined, which is presented in **Table 6**.

The results in **Table 6** indicate that the average energy required to produce one ton of bentonite product (finer than 75 microns) was calculated to be 48 kWh. In order to measure the tonnage of material flow rate and energy in different parts of plant, it was measured during 4 times with 4-hour intervals, and its average was recorded as the material flow rate. Then, by referring to the control room and electrical panels, and measuring the frequencies (ampere) consumption values for each device during 4 times, the average electrical ampere was determined to calculate the power consumption in kilowatts. Then, the material and energy balance in the comminu-

Table 7. Material and energy balance of different parts of the production line

	Energy consumption (kWh)	Material flow rate (t/h)	Energy consumption for 1 ton (kWh)	Percentage share of total consumption
Hammer mill	25.2	9	2.8	5.9
Tube mill	102	5.5	18.5	38.5
classifiers	54	5.5	9.8	20.4
Fine-grained part of classifiers		2.2		
Coarse-grained part of classifiers		3.3		
Other parts (fans, cyclones, conveyors, elevators, etc.)	----	----	16.9	35.2
The whole set of grinding line	----	----	48	100

tion circuit was examined. A summary of the results is presented in **Table 7**.

3.2. Net power of the mill using Morrell and Austin models

Since it is not possible to measure the net power of the mill on site, therefore, using **Equations 5** to **9** and also **Equations 10** to **14** (**Austin, 1990**), first some parameters of **Table 8** were determined and then the values of α, ρ_c, P_t and P_e were obtained as 0.167, 3.8 t/m^3, 66.3 kW and 15.8 kW, respectively. Finally, the net power of the tube mill was calculated as 50.5 kW. Therefore, the ratio of net power (50.5) to gross power (66.3) was obtained as 76%, which will be applied in calculations related to the operational work index.

Table 8. Parameters required in Morrell and Austin relations

Inside diameter of the mill (m)	D_m	1.54
Effective length of the mill (m)	L_e	5.2
Specific weight of the load (t/m^3)	ρ_c	3.8
Calibration constant	K	9.1
Length of the cylindrical section of the mill (m)	L_d	5.2
Speed of the mill relative to the critical speed	φ_c	0.79
Part of the mill occupied by the total load	J_t	0.214
Factor related to the relative degree of filling	A	0.167
Factor related to the speed of rotation	Δ	0.75

$$\alpha = J_t(1 - 1.03J_t) \tag{10}$$

$$\delta = \varphi_c\left[1 - \left({}^{0.1}/_{2^{9-10\varphi_c}}\right)\right] \tag{11}$$

$$\rho_c = \frac{(1-\varphi)J_t\left(\frac{\rho_R}{M_R}\right) + 0.6\,J_B\left(\rho_b - \frac{\rho_R}{M_R}\right)}{J_t} \tag{12}$$

$$P_t = KD_m{}^{2.5}L_e\rho_c\alpha\delta \quad \text{kW} \tag{13}$$

$$P_e = 1.68D_m{}^{2.5}[\varphi_c(0.667L_d + L)]^{0.82} \tag{14}$$

In order to determine the maximum value of **α**, the derivative of **Equation 10** with respect to J_t is set equal to zero (**Equation 15**).

$$\alpha' = 0 \rightarrow 1 - 2.06J_t = 0 \rightarrow J_t = 0.485 \tag{15}$$

The value of α_{max} by using $J_t = 0.485$, is 0.243.

3.3. Efficiency of the comminution circuit

In order to optimize the comminution circuit, the entire circuit must be evaluated and the criterion for this evaluation is the calculation of the efficiency of each device. Therefore, this decision was made that at the beginning, with the efficiency of tube mill to be calculated. Next, the efficiency of the closed grinding circuit (tube mill and classifier) was investigated and finally, the efficiency of the hammer mill (primary crushing) was studied.

3.3.1. Efficiency of the tube mill

By referring to the plant electrical and control panel, the average frequency consumption (ampere) of the tube mill was measured over 4 days which was 170 amperes. According to the phi in **Equation 16**, the power consumption of the mill's dynamo was calculated to be 102 kW (0.6 kW of energy is consumed per ampere) (**Abdulkareem et al., 2021**).

$$p = \sqrt{3}VI\cos\emptyset \tag{16}$$

Where:

p – the power consumption (kW),
V – the 3-phase electrical voltage in volts which is approximately 380 v,
I – the current consumption of the device in amperes,
cos Ø – considered to be 0.9 according to the technical specifications of the dynamo.

Table 9. Parameters required to calculate the ball mill operating work index

Mill feed size	3350 µm
Mill product size	380 µm
Mill feed Tonnage	5.5 t/h
Measured power	102 kW
* Pure power	77.5 kW

* The net power is achieved by multiplying the measured power by the factor 0.76 (net power/measured power=0.76).

According to the data in **Table 9** and the power consumption of the tube mill (102 kW), the operational work index was obtained from **Equation 17** as 37.7 kWh/t.

$$w_{i(op)} = \frac{W}{Q\left(\frac{11}{\sqrt{P_{80}}} - \frac{11}{\sqrt{F_{80}}}\right)} \tag{17}$$

Where:

$w_{i(op)}$ – operating work index (kWh/t),
Q – mill feed flow rate (t/h),
P_{80} – Mill product size (microns),
F_{80} – Mill feed size (microns),
W – net power (kW).

In order to calculate the efficiency of the mill, the ratio of the laboratory work index $w_{i(lab)}$ to the operational work index $w_{i(op)}$ should be used (**Equation 18**) (**Wikedzi, 2020**).

$$EF = \frac{W_{i(lab)}}{W_{i(op)}} \tag{18}$$

The calculated operational work index cannot be directly included in the efficiency equation because it is not comparable with the laboratory work index. For this purpose, some coefficients must first be applied to achieve the normalized work index value. These coefficients include the circuit dryness coefficient (1.3), the ball mill closed circuit coefficient (1), the circulating load coefficient (1.05), the mill diameter coefficient (1.1), the particle fineness coefficient (1.06), the crushing ratio coefficient (1), and the coefficient related to energy losses (1.2). By applying these coefficients, the operational work index was obtained as 19.7 kWh/t. Finally, the efficiency value (the ratio of the laboratory work index to the operational work index) was calculated as 32%.

3.3.2. Efficiency of the grinding Circuit

The efficiency of the grinding circuit depends on two factors: the efficiency of the grinding operation and the efficiency of the classification system. In other words, a greater match between the grinding product and the classifier separation limit indicates a greater efficiency of the operation. Given that the grinding circuit consists of mills and classifiers, the sum of the measured powers of the mills and classifiers was used as the circuit consumed power in the Bond relation.

3.3.2.1. Consumed power of the classifier

By referring to the control room, the power consumption of each classifier was measured 4 times at 4-hour intervals and the average was 45 amperes. According to **Equation 16**, the consumed power of the device was obtained as 27 kWh. The solid flow rate of 2.75 t/h was considered for the classifier, therefore the share of energy consumed by all classifiers to produce one ton of product was calculated as 9.8 kWh. Moreover, the energy consumption of the classifier in the no-load state was obtained as 15.8 kWh by **Equation 7**.

Table 10. Parameters required to calculate the operating work index of the tube mill

Feed size	8500 μm
Product size	48 μm
mill Circuit Capacity	2.2 t/h
*Pure Power of mill	77.5 kWh
consumed Power of classifiers	54 kWh

* Net power is obtained by multiplying the measured power by a factor of 0.76.

According to **Table 10** and **Equation 16**, the operating work index of the tube mill circuit was calculated to be 40.7 kWh/t, and by applying the relevant coefficients, it was calculated to be 21.3 kWh/t, and finally its efficiency coefficient was 30%.

3.3.3. Efficiency of the hammer mill

According to the size distribution tests, the d_{80} of the feed and product of the hammer mill were estimated as 72 and 8.5 mm, respectively. By referring to the electrical panel of the machine and measuring the amount of consumed electricity, the power consumption of the machine was calculated as 42 amperes, equal to 25.2 kWh. Using the empirical formula of the Bond and the tonnage of the hammer mill feed (9 t/h), the operational work index at this stage was estimated as 35.8 kWh/t. In this regard, the correction factor for the dryness of the mill circuit was considered as 1.3 and the correction factor related to energy losses (same as impact crusher) (**Wills, 1997**) was considered as 1.6. Therefore, the operational index was calculated as 17.2 kWh/t. As a result, in the next stage, the hammer mill efficiency coefficient, which is the ratio of the laboratory to the operational work index, was obtained as 37.03%.

3.4. Circulating load and its effect on the circuit

3.4.1. Circulating load measurement

In order to measure the circulating load, the sliding door under the classifier screw was opened for 10 minutes and the coarse part of the classifiers was collected, which was 550 kg. Therefore, the circulating load tonnage was obtained as 3300 kg/h and equal to 150%, or a coefficient of 1.5.

3.5. Classifier Efficiency

The efficiency of the classifier was obtained using **Equation 19** and considering parameters values, was equal to 66.3%. Also, based on the results of the classification of coarse and fine parts of classifier samples, the values of the distribution coefficient in different classification ranges were calculated, which are presented in **Table 11** and **Figure 4**. In addition, using **Equation 20**, the calculated circulating load was equal to 300%.

$$E = \frac{v(f-u)(1-u)(v-f)}{f(v-u)^2(1-f)} \quad (19)$$

$$CL = \frac{u-f}{f-v} \quad (20)$$

Where:

E – classifier efficiency (%),

CL – calculated circulating load (%),

f – percent of material coarser than the cut size in the initial load, classifier feed (65.6),

v – percent of material coarser than the cut size in the coarse part of the classifier (85.3),

u – percent of material coarser than the cut size in the fine part of the classifier (6.6).

Table 11. Determining the classifier distribution coefficient

Size fraction (µm)	Average size (µm)	Weight of coarse part (g)	Weight of fine part (g)	Distribution coefficient (%)
+1180	-	9.9	-	100
+710-1180	945	17.3	-	100
+500-710	605	24.1	-	100
+355-500	427	22.9	-	100
+250-355	302	33.6	-	100
+177-250	213	48.9	-	100
+150-177	163	37.5	0.5	98.7
+105-150	127	77.8	7	91.7
+74-105	89	28.9	7.9	78.5
+44-74	59	36.6	37.7	49.3
-44	-	15.1	186.7	7.4
-	-	352	236	-

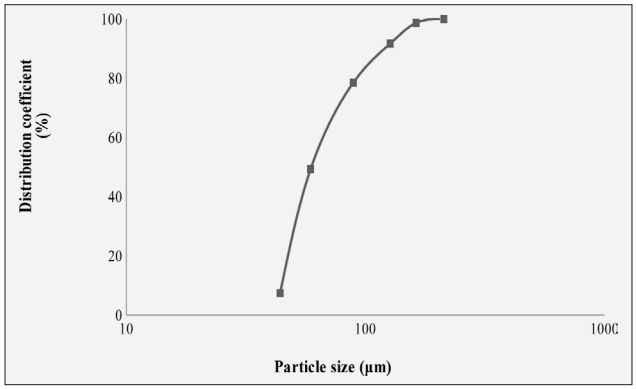

Figure 4. Classifier distribution coefficient curve

It is worth noting that the main reason for the discrepancy between the measured and calculated circulating load is the segregation of particles which happens inside the classifier. About 5% of the incoming load to the classifier, due to the agglomeration of fine particles to each other, and the creation of particles in size fractions of -1180 and +710 microns, which are broken again, and therefore are transferred to finer fractions. According to the distribution coefficient curve in **Figure 4** and calculations related to the efficiency of the classifier, the operating parameters of the classifiers are given in **Table 12**.

3.6. Effect of agglomeration on the grinding circuit

Agglomeration in bentonite is the process where individual clay particles come together to form larger, loosely bound clusters or aggregates. This phenomenon reduces the purity of the product and creates a wide particle size distribution (**Zhang et al., 2024**). At the outlet of the tube mill and circulating load, the agglomerated particles of **Figure 5** constitute about 90% of the fractions coarser than 500 microns. This increases the weight of

Table 12. Operating parameters of classifiers at the Arak micronized powder plant

Separation limit	d_{50}	60 µm
Defect coefficient	$\frac{d_{75} - d_{25}}{2 \times d_{50}}$	0.31
Accuracy index	$\frac{d_{25}}{d_{75}}$	0.56
Fine part tonnage (product)	-	2.2 t/h
Coarse part tonnage (circulating load)	-	3.3 t/h
Measured circulating load	-	150 %
Ideal circulating load	-	190 %
Efficiency	-	66.3 %

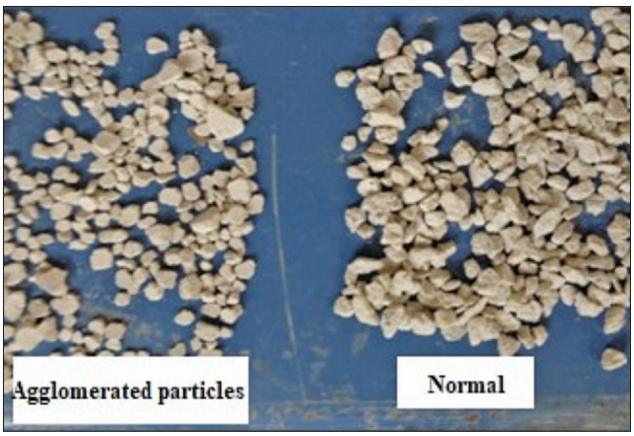

Figure 5. Comparison of agglomerated particles 0.5 to 3 mm with normal particles

the particles with coarser sizes to the mill, reduces the grinding efficiency, and causes regrinding, as well.

In these classifiers, the sizes of some particles are reduced due to the following reasons:

- Direct collision of particles with blades,
- Softness of minerals (bentonite),
- Looseness and softness of particles in the initial or parent fractions of the particles that are formed due to the agglomeration phenomenon.

The breakage which carried out in the classifier neutralizes the agglomeration process and reduces the percentage of coarse particles in the circulation load and, as a result, increases the efficiency of the grinding circuit. This is clearly evident in the size fractions of +1180 and +710-1180 of the tube mill product and the coarse part of the classifiers. However, the d_{80} of coarse part of the classifier is almost equal to the d_{80} of mill's product, instead of being coarser.

3.7. Effective parameters in optimization

According to the measurement and calculation of the power and energy consumption of different devices, and the determination of the grinding circuit efficiency, the changeable parameters are examined below.

Table 13. Effect of changes in the size of the tube mill's feed on the efficiency of the grinding circuit

	Efficiency (%)	Corrected Operating Work Index (kWh/t)	Operating work index (kWh/t)	Average size of balls (mm)	Feed size (µm)
Row	E	D	C	B	A
1	5.1	123.8	301.3	0.06	1000
2	14.6	43.8	106.5	0.06	2000
3	26.7	23.9	58.0	0.06	3000
4	41.1	15.5	37.7	0.06	4000
5	57.4	11.1	26.9	0.06	5000
6	75.8	8.4	20.5	0.06	6000
7	95.1	6.7	16.3	0.06	7000
8	115.8	5.5	13.3	0.06	8000

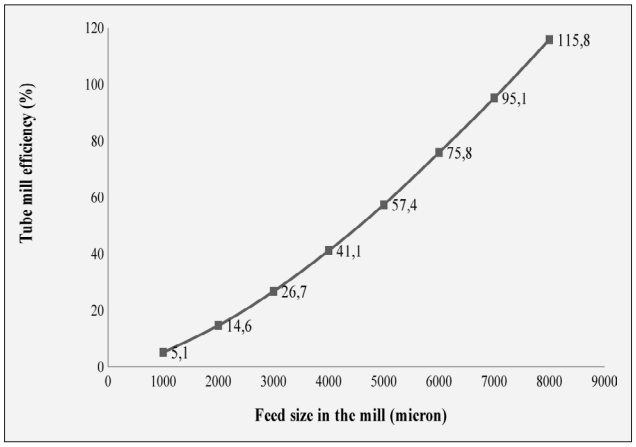

Figure 6. The effect of changes in the size of the mill feed on the efficiency of the grinding circuit

3.7.1. Effect of mill feed size on the grinding circuit efficiency

In this section, by applying changes to the size of tube mill's feed and referring to the Bond relation, and assuming that other parameters such as mill dimensions, rotation speed, ore density and ball diameter remain constant, the operational work index was directly calculated. Referring to **Table 13** and **Figure 6**, the following results were accordingly achieved:

- Under the current operating conditions of the tube mill: 80 to 40 mm balls diameter, specific gravity of 1500 kg/m^3, mill diameter of 1.54 m and relative rotation speed of 79%, the conditions of comminution circuit would be convenient (work index of 20 kWh/t). Considering the work index, it could clearly be postulated that this is in contrast to the characteristics of bentonite, which is a soft material. Therefore, by increasing the size of the feed entering to tube mill, the conditions for grinding soft materials (work index lower than 7 kWh/t) can be changed.
- By increasing the size of the feed entering to tube mill from 3000 microns to 7000 microns, the efficiency of the mill increases linearly up to 60%.

According to **Equation 21** (the equation for calculating the maximum diameter of the ball), the operating work index was calculated by **Equation 22** which was 301.3 kWh/t. Using the correction coefficients (F_1, F_3, F_4, F_6 and F_8 described earlier) and their multiplication (which was 1.91), the corrected operating work index from **Equation 23** (0.78Δ) was 123.8 kWh/t, and finally the efficiency from **Equation 24** was 0.0514 or 5.14%.

$$B = K \times F^{0.5} \times \left(\frac{\sigma \times W_i}{100 \times C_s \times \sqrt{D}}\right)^{\frac{1}{3}} \quad (21)$$

Where:

B – Ball diameter (m),
w_i – Ore work index (6.37 kWh/st),
F – Input charge size (based on 80% passing) in meters (0.0034 m),
σ – Ore density in kg/m^3 (1500 kg/m^3),
D – Mill internal diameter (1.45 m),
C_s – Mill rotation in terms of critical speed (0.79),
K – Constant value (equal to 0.114 for dry grinding and 0.111 for wet grinding).

$$C_1 = W_i = \frac{100 \times C_s \times \sqrt{D} \times B^3}{\sigma \times K^3 \times F^{1.5}} \quad (22)$$

$$D_1 = W_{i_c} = \frac{W_i \times \Delta}{F_1 \times F_3 \times F_4 \times F_6 \times F_8} \quad (23)$$

$$E_1 = \frac{6.37}{D_1} \quad (24)$$

3.7.2. Effect of ball sizes on the tube mill efficiency

To study on the effect of ball size on the tube mill efficiency, the optimal and necessary diameter of ball was first calculated and then compared with the diameter of the used balls. According to the Bond ball relation, by changing the ball diameter and keeping the other physi-

cal parameters of the mill constant, the changes in the work index were examined. To calculate the maximum diameter, **Equation 21** was used and it was equal to 0.031 m.

Therefore, the maximum optimal diameter of the mill's balls was considered to be 40 mm. The mixture of the proposed balls is given in **Table 14**.

Using **Equation 25** and setting the value of 0.03 for B, 0.0034 for F, 0.114 for K, and 0.79 for C_s, the work index value was estimated as 6.1 kWh/t. Similarly, by including the various correction coefficients which was 1.91, the corrected work index was calculated 2.5, using **Equation 26** (Δ = 0.78). Finally, the efficiency coefficient was calculated 254.8%, using **Equation 27**.

$$C_1 = W_i = \frac{100 \times C_s \times \sqrt{D} \times B^3}{\sigma \times K^3 \times F^{1.5}} \quad (25)$$

$$D_1 = W_{i_c} = \frac{W_i \times \Delta}{F_1 \times F_3 \times F_4 \times F_6 \times F_8} \quad (26)$$

$$E_{1=} \frac{6.37}{2.5} = 254.8\ \% \quad (27)$$

Referring to **Table 15** and **Figure 7**, it can be concluded that by reducing the average size of the balls to 40 and 30 mm, the efficiency of the mill increases exponentially by 55 and 107%, respectively. Therefore, it is suggested to use balls with an average diameter of 40 mm instead of 60 mm, whereby the tube mill efficiency will increase by 55%.

3.7.3. Effect of production capacity on the tube mill efficiency

In this section, by placing the capacities in the Bond relation, and assuming that the parameters of the feed and product sizes and the work index remain constant, the ideal power consumption was accordingly calculated. Then, using the scale conversion factor, the amount of operational consumed power of the device in the real state was estimated. Finally, the operating work index was determined and the related efficiency was accordingly calculated. The results of these changes are presented in **Table 16** and **Figure 8**.

Considering that the tonnage of charge entering to the mill is 2.5 times of the production capacity, the following calculations are accordingly made (**Equations 28-32**):

$$B_1 = A + A \times 1.5 = A \times 2.5 = 1 \times 2.5 = 2.5\ t/h \quad (28)$$

$$C_1 = B_1 \times W_i \times \left(\frac{11}{\sqrt{380}} - \frac{11}{\sqrt{3350}}\right) = $$

$$= 2.5 \times 6.37 \times 0.374 = 5.9\ kWh \quad (29)$$

$$D_1 = C_1 \times 5.9 = 34.8\ \ kWh \quad (30)$$

$$E_1 = \frac{D_1}{B_1\left(\frac{11}{\sqrt{380}} - \frac{11}{\sqrt{3350}}\right) \times F_1 \times F_3 \times F_4 \times F_6 \times F_8} =$$

$$= \frac{34.8}{2.5\left(\frac{11}{\sqrt{380}} - \frac{11}{\sqrt{3350}}\right) \times 1.91} = 19.5\ \frac{kWh}{t} \quad (31)$$

$$F_{1=} \frac{6.37}{E_1} = 32.6\ \% \quad (32)$$

Based on the results in **Table 16**, it can be postulated that changing the production capacity, while keeping other parameters constant, does not have a significant effect on the grinding system efficiency.

3.7.4. Effect of filling on the tube mill efficiency

According to the measurements inside the tube mill, the material height and the balls surface are 112 and 121 centimeters, respectively. Therefore, using **Equation 33**, the percentage of filling of the materials and the balls were estimated as 21.4 and 14% for the materials and the balls, respectively. In **Equation 33**, D and H are the inside diameter of the mill, and the distance between the

Table 14. Comparison of used and estimated balls

Diameter of used balls (mm)	Estimated balls diameter (mm)	Estimated balls weight %
85	---	---
55	40	51%
40	25	49%

Table 15. Effect of changing ball dimensions on tube mill efficiency

	Efficiency (%)	Corrected Operating work index (kWh/t)	Operating work index (kWh/t)	Feed size (µm)	Average diameter of balls (m)
Row	E	D	C	B	A
1	254.8	2.5	6.1	3350	0.03
2	107.9	5.9	14.2	3350	0.04
3	55.4	11.5	27.8	3350	0.05
4	32.2	19.8	48.1	3350	0.06
5	20.3	31.4	76.3	3350	0.07
6	13.6	46.8	113.9	3350	0.08

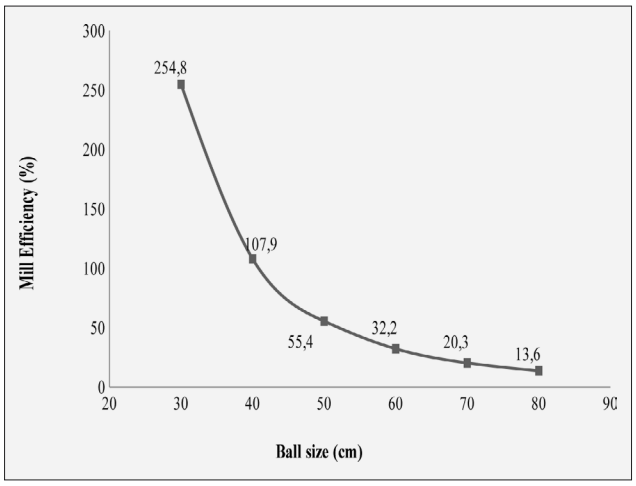

Figure 7. Effect of changing the size of the balls on the efficiency of the tube mill

$$B_1 = \delta = \varphi_c\left[1 - \left({}^{0.1}/_{2^{9-10\varphi_c}}\right)\right] =$$

$$= 0.79\left[1 - \left({}^{0.1}/_{2^{9-7.9}}\right)\right] = 0.75 \quad (34)$$

$$C_1 = \alpha = J_t(1 - 1.03J_t) =$$

$$= A_1 \times (1 - 1.03 \times A_1) = 0.09\ kW \quad (35)$$

$$D_1 = P_t = KD_m{}^{2.5}L_e\rho_c\alpha\delta =$$

$$= 9.1 \times 1.54^{\cdot 2.5} \times 5.2 \times 3.8 \times 0.09 \times 0.75 = 35.7\ kW \quad (36)$$

$$P_e = 1.68 \times 1.54^{2.5}[0.79 \times 5.2]^{0.82} = 15.8\ kW \quad (37)$$

$$E_1 = D_1 - 15.8 = 19.9\ kW \quad (38)$$

Table 16. The effect of changes in production capacity on mill's efficiency

	Efficiency (%)	Operating work index (kWh/t)	Estimated net operating power (kW)	Ideal power (kW)	Incoming tonnage to mill (t/h)	Production capacity (t/h)
Row	**F**	**E**	**D**	**C**	**B**	**A**
1	32.6	19.5	34.8	5.9	2.5	1
2	32.6	19.5	52.7	8.1	3.75	1.5
3	32.6	19.5	70.2	10.8	5	2
4	32.6	19.5	87.8	13.5	6.25	2.5
5	32.6	19.5	105.3	16.2	7.5	3
6	32.6	19.5	122.9	18.9	8.75	3.5
7	32.6	19.5	140.5	21.6	10	4

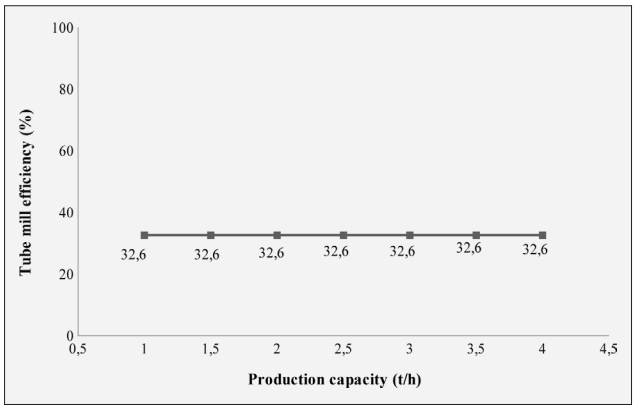

Figure 8. Impact curve of changes in production capacity on mill's efficiency

surface of the balls and to the upper point of the mill, respectively.

$$113 - 126\frac{H}{D} \quad (33)$$

Therefore, the percentage of the mill charge, based on the measurement of the material bed height, is 21.4% for each of the mill chambers.

$$F_1 = E_1 \times 1.5 = 29.9\ kW \quad (39)$$

$$G_1 = \frac{F_1}{5.5\left(\frac{11}{\sqrt{380}} - \frac{11}{\sqrt{3350}}\right) \times 1.91} = 7.6\ \frac{kWh}{t} \quad (40)$$

$$H_1 = \frac{6.37}{G_1} = 83.8\ \% \quad (41)$$

According to the Austin relations, the effect of changes in the mill filling from 10 to 85% on the efficiency were calculated, using **Equations 34-41** and are given in **Table 17** and the calculated values of efficiencies versus mill filling are presented in **Figure 9**. According to **Figure 9** and **Table 17**, the following results were achieved:

- With increasing mill filling, the efficiency decreases and reaches to its minimum level at 48.5% and increases thereafter, as well.
- The rate of change in efficiency at low filling (10-15%) or high filling (75-80%) is much higher than at medium filling.
- By comparing rows 3 and 9 in **Table 17**, it can be postulated that the amount of energy consumed at

Table 17. Effect of changes in ball and powder loading on mill efficiency

	Efficiency (%)	Operating work index	Estimated net operating power (kW)	Net power (kW)	Gross power (kW)	Coefficient α	Coefficient δ	Percentage of filling
Row	H	G	F	E	D	C	B	A
1	83.8	7.6	29.9	19.9	35.7	0.09	0.75	10
2	48.3	13.2	51.8	34.5	50.4	0.127	0.75	15
3	35.4	18	71	47.3	63.1	0.159	0.75	20
4	24.8	25.7	101.3	67.5	83.3	0.21	0.75	30
5	21.5	29.6	116.4	77.6	93.4	0.235	0.75	40
6	20.7	30.7	120.5	80.3	96.1	0.242	0.75	50
7	22.2	28.7	112.8	75.2	91	0.229	0.75	60
8	27.0	23.6	92.6	61.7	77.5	0.195	0.75	70
9	32.2	19.8	77.9	51.9	67.7	0.171	0.75	75
10	41.6	15.3	60.2	40.1	55.9	0.141	0.75	80
11	63.7	10	39.3	26.2	42	0.106	0.75	85

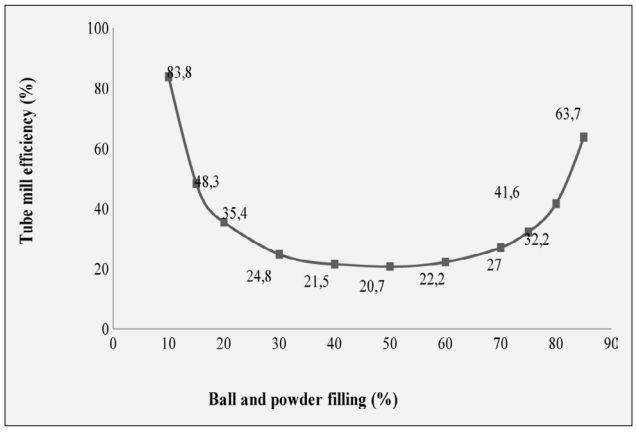

Figure 9. Tube mill efficiency variation curve based on percentage of filling

20% and 75% filling is almost equal (35.4% and 32.2%). Therefore, by increasing the ball and materials filling to 75% and assuming that the particles residence time inside the mill remains constant, the capacity and ultimately the efficiency (indirectly) increases by up to 3 times (by 60%) without the need for more energy consumption.

3.7.5. Calculation of the ideal tube mill filling

By considering the laboratory Bond work index as the ideal value and the capacity of 5.5 t/h and assuming that the sizes of feed and product are constant, the ideal energy consumption of the tube mill was achieved using **Equations 42** and **43**.

$$P = 5.5\left[6.37\left(\frac{11}{\sqrt{380}} - \frac{11}{\sqrt{3350}}\right)\right] = 13.1\ \left(\frac{kWh}{t}\right) \quad (42)$$

$$P_c = P \times 1.3 \times 1.05 \times 1.1 \times 1.06 \times 1.2 = 25.1\ \left(\frac{kWh}{t}\right) \quad (43)$$

The ideal consumed energy value is considered in Austin relation, and assuming that other parameters are constant, the ideal filling rate of the tube mill was accordingly calculated as follows, using **Equations 44-46**:

$$P_c = P_t - P_e \quad (44)$$

$$KD_m{}^{2.5}P_cL_e\rho_c\alpha\delta - 15.8 = 25.1 \quad (45)$$

$$\alpha = 0.103\ = J_t(1 - 1.03J_t) \rightarrow J_t = 88\%\ \&\ 12\% \quad (46)$$

Thus, referring to whole calculated values, it can be seen that theoretically, by applying 12 and 88 percent of charge and ball filling, the ideal consumed energy can be achieved.

3.7.6. Effect of relative rotation speed on the tube mill efficiency

The measured tube mill rotation speed was 26 rpm. The inside mill diameter is 1.54 m, and as a result, the critical speed is 34.1 rpm (**Equation 47**). If the ratio of the mill rotation speed to the critical speed is considered 79% (**Wills, 1997**), the rotation speed was calculated to be 27 rpm, which is almost equal to the measured one (26 rpm).

$$N_c = \frac{42.3}{\sqrt{1.54}} = 34.1 \quad (47)$$

Using Austin's equation, the effect of relative percentage changes in mill rotation speed from 40 to 100% on consumed power and mill efficiency were calculated using **Equations 48-55**, which are presented in **Table 18** and the graph in **Figure 10**.

$$B_1 = \delta = \varphi_c\left[1 - \left({}^{0.1}/_{2^{9-10\varphi_c}}\right)\right] = 0.4 \quad (48)$$

Table 18. Effect of rotation speed on mill efficiency

	Efficiency (%)	Operating work index (kWh/t)	Estimated net operating power (kW)	Net power (kW)	No-load power (kW)	Gross power (kW)	α value	δ value	Circulation speed (φ_c)
Row	I	H	G	F	E	D	C	B	A
1	63.1	10.1	29.3	26.4	9.0	35.4	0.167	0.4	40
2	49.8	12.8	50.1	33.4	10.8	44.2	0.167	0.5	50
3	41.4	15.4	60.6	40.4	12.6	53.0	0.167	0.6	60
4	35.0	18.2	71.4	47.6	14.3	61.9	0.167	0.7	70
5	32.2	19.8	77.8	51.9	15.3	67.2	0.167	0.76	80
6	30.1	21.2	83.3	55.5	16.1	71.6	0.167	0.81	90
7	30.5	20.9	82.2	54.8	15.9	70.7	0.167	0.8	100

$$C_1 = \alpha = J_t(1 - 1.03J_t) =$$

$$= 0.214 \times (1 - 1.03 \times 0.214) = 0.167 \text{ kW} \quad (49)$$

$$D_1 = P_t = KD_m{}^{2.5}P_cL_e\rho_c\alpha\delta =$$

$$= 9.1 \times 1.54^{2.5} \times 5.2 \times 3.8 \times 0.167 \times 0.4 = 35.4 \text{ kW} \quad (50)$$

$$E_1 = P_e = 1.68 \times 1.54^{2.5}[0.4 \times 5.2]^{0.82} = 9.0\ kW \quad (51)$$

$$F_1 = D_1 - E_1 = 26.4 \text{ kW} \quad (52)$$

$$G_1 = E_1 \times 1.5 = 39.6 \text{ kW} \quad (53)$$

$$H_1 = \frac{F_1}{5.5\left(\frac{11}{\sqrt{380}} - \frac{11}{\sqrt{3350}}\right) \times 1.91} = 10.1 \frac{\text{kWh}}{\text{t}} \quad (54)$$

$$I_{1=}\frac{6.37}{H_1} = 57.3\ \% \quad (55)$$

According to **Figure 10** and **Table 18**, the following results were achieved:

- By reducing the relative rotation speed of the mill from 100 to 80%, there is no significant change in energy consumption.
- By reducing the relative rotation speed of the mill from 80 to 40%, the energy consumption decreases exponentially with a slow slope, and as a result, the efficiency increases by increasing the abrasion mechanism in the mill.
- By changing the relative rotation speed of the mill from the current 79% to 60 to 50%, the mill efficiency increases by 15%.

3.7.7. Average residence time

In order to measure the particles average residency time in the mill, the volume of material inside the mill was divided by the capacity of the mill. By measuring the height of the material and the balls, the volume of the sum of these two was calculated, and considering the tonnage and density of the balls, the volume of the balls was subtracted from this value and the volume of material inside the mill was adjusted accordingly. Therefore, the apparent volume of the balls and the sum of the powder and balls were calculated, using **Equation 33** as 1.3 and 2 m^3, respectively. If the volume of the empty space between the balls is considered to be 40% (**Arjmand et al., 2012**), the actual volume of the powder inside the mill is 1.22 m^3 and the volume of powder flow in the mill (is the ratio of the capacity to the apparent density of the ore), is 4.4 m^3/h. Therefore, the particle residence time was calculated as the result of dividing the actual volume of powder inside the mill (1.22) by the volume of powder flow in the mill (4.4), which would be 0.28 h (16.6 min). Given that reducing the residence time indirectly reduces energy consumption, mill efficiency can accordingly increase by reducing the residence time.

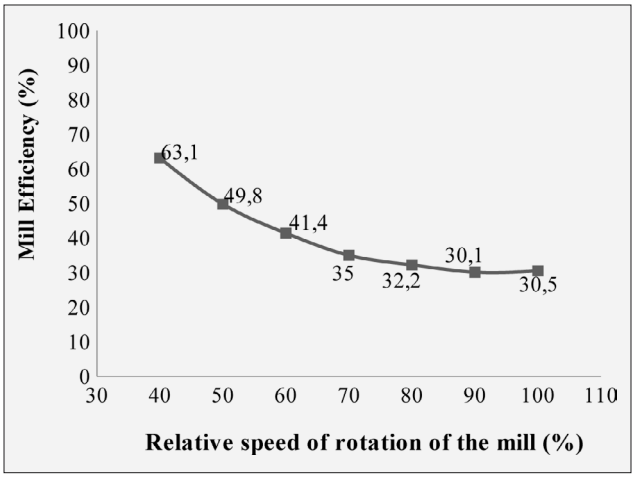

Figure 10. Curve of the effect of rotation speed on the efficiency of the mill

4. Conclusions

According to the measurements, tests and calculations carried out on the Arak Company's comminution circuit using bentonite, the following results and suggestions are presented:

- The efficiency of the comminution system was determined to be about 30%, which is very low and urgently needs troubleshooting and optimization.
- 48 kWh of energy is consumed to break one ton of feed with product size finer than 75 μm. 59% of this amount is related to the tube mill.
- The average diameter of the steel balls used is 60 mm, which is larger than the optimal and calculated ball diameter, and it is better to use smaller balls with a maximum diameter of 50 mm in the first chamber and 30 mm in the second chamber. In this case, the mill efficiency will increase by 50%.
- Changing the production capacity, keeping other parameters constant, will not effect on the efficiency of the grinding system.
- By reducing the relative rotation speed of the mill from the current 79% to 50-60%, the energy consumption is reduced exponentially with a slow slope, and as a result, by increasing the abrasion mechanism in the mill, the efficiency increases by 15%.
- By increasing the filling amount of the first and second chambers in tube mill, by 60 and 70%, respectively, the abrasion mechanism will increase. As a result, the capacity increases with no more energy, and the efficiency increases by 60%.
- By increasing the tube mill size from 3000 to 7000 μm, the mill efficiency increases linearly by 60%.
- The tube mill circulating load was 150%, which suggests an increase to the ideal circulating load (190%).
- About 16% of the coarse particles, in tube mill product, are agglomerated pieces. Therefore, reducing this phenomenon will have a direct impact on reducing energy consumption and increasing efficiency.
- In order to reduce agglomeration, additives can be used to prevent materials from sticking to each other and thus increase mill efficiency. Among the additives, and for further study, cellophane, calcium stearate, polyphenol, alcohol, acetate, glycol, amine and even water would be tested.

Therefore, the changes in tube mill circulating load, the filling amount of the first and second chambers, the tube mill size, energy consumption of the tube mill, average diameter of the steel balls of the first and second chambers, respectively have the greatest impact on improving the efficiency of the grinding process.

5. References

Abdulkareem, A., Somefun, T. E., Oguntosin, V., Ogunade, F. (2021). Development and construction of automatic three-phase power changeover control circuit with alarm, In *IOP Conference Series: Materials Science and Engineering*, *1036* (1), p. 012081, IOP Publishing. https://doi.org/10.1088/1757-899X/1036/1/012081

Alsaeed, R. D., Alaji, B., Ibrahim, M. (2022). Using bentonite clay as coagulant aid for removing low to medium turbidity levels, *Iranian Journal of Chemistry and Chemical Engineering*,*41*(12).doi:10.30492/IJCCE.2022.535532.4873

Arjmand, G., Shafaee, S. Z., Noparast, M., Farzanegan, A., Gafari, N. (2012). Determination and Scale-up of Specific Rate of Grinding of Placer Iron Ore of Sangan. *Journal of Mining Engineering*, *6*(13), 61-69. doi: 20.1001.1.17357616.1390.6.13.6.3

Asa'd, O., Levesque, M. (2024). Digital technologies for energy efficiency and decarbonization in mining, *CIM Journal*, *15*(1), 1-20. doi:10.1080/19236026.2023.2203068

Austin, L. G. (1990). A mill power equation for SAG mills, *Mining, Metallurgy & Exploration*, *7*, 57–63. https://doi.org/10.1007/BF03403284

Austin, L.G., Klimple, R.R., Luckie, P.T. (1984). Process Engineering of Size Reduction: Ball Milling, *Society of Mining Engineers*, AIME, USA.

Bentonite, K. A. O. L. I. N. (2005). Bentonite, kaolin, and selected clay minerals, *Identity*, *2*, 1, World Health Organization Geneva. https://iris.who.int/handle/10665/43102

Bian, X., Wang, G., Wang, H., Wang, S., Lv, W. (2017). Effect of lifters and mill speed on particle behaviour, torque, and power consumption of a tumbling ball mill: Experimental study and DEM simulation, *Minerals Engineering*, *105*, 22-35. doi:10.1016/j.mineng.2016.12.014

Bogdanov, V. S., Bogdanov, D. V., Sychev, E. A., Karachevtseva, A. V. (2022). Calculation of the Parameters of the Grinding Load in a Ball-Tube Mill for the Production of Construction Materials, *International Scientific Conference on Innovations and Technologies in Construction*, 180-188, Cham: Springer International Publishing. doi:10.1007/978-3-031-20459-3_23

Bond, F.C. (1961a). Crushing & Grinding Calculations, Part I, *British Chemical Engineering*, *6*(6), 378-385. doi:10.4236/ijg.2013.47099

Bond, F.C. (1961b). Crushing & Grinding Calculations, Part II, *British Chemical Engineering*, *6*(8), 543-547.

Chimwani, N., Bwalya, M. M. (2021). Milling studies in an impact crusher I: kinetics modelling based on population balance modelling, *Minerals*, *11*(5), 470. doi: 10.3390/min11050470

Dehghan, A. A., Pourkarimi, Z., Nouparast, M., Shafiei, S., Jorjani, E. (2008). Evaluation of grinding circuit performance in Esfordi phosphate processing plant, *Iranian Journal of Science and Technology Transaction B-Engineering*, *32* (4), 415-424. http://irdoi.ir/929-413-277-146

Dehghani, A., Parandeh, L., Khosravi-Rad, M., Noaparast, M. (2016). Verification of MODSIM ball mill and hydrocyclone models for Se-Chahun grinding circuit. *Journal of Mining Engineering*, *11*(30), 13-20. doi: 20.1001.1.17357616.1395.11.30.2.8

Elbendari, A. M., Ibrahim, S. S. (2025). Optimizing key parameters for grinding energy efficiency and modeling of particle size distribution in a stirred ball mill, *Scientific Reports*, *15*(1), 3374. doi:10.1038/s41598-025-87229-8

Fuerstenau, M., Han, K.N. (2003). Principles of Mineral Processing, Published by SME. doi: 10.4236/eng.2013.510B002

Golpayegani, M. H., Rezai, B. (2022). Modelling the power draw of tumbling mills: A comprehensive review, *Physicochemical Problems of Mineral Processing*, *58*(4). doi: 10.37190/ppmp/151600

Grim, R. E., Guven, N. (2011). Bentonites: geology, mineralogy, properties and uses, *24*, Elsevier. https://doi.org/10.37190/ppmp/151600

Kelly, E.G., Spottiswood, D.J. (1989). Magnetic separation. Introduction to Mineral Processing, Printed in Australia by Lamb Printers, 274-290.

Khan, A. S., Khan, A. A., Ali, S. U., Javed, A., Farman, M. (2025). Optimizing coal mill for efficient Thar lignite utilization, *International Journal of Coal Preparation and Utilization*, 1-25.

Khurmamatov, A., Mukhamedbaev, A. (2023). Intensifying the cement grinding process, *E3S Web of Conferences*, *402*, p. 14035, EDP Sciences. doi: 10.1051/e3sconf/202340214035

Kutlić, A., Bedeković, G., Sobota, I. (2012). Bentonite processing, *Rudarsko-geološko-naftni zbornik*, *24*(1), 61-65. https://hrcak.srce.hr/107809

Lamrani, M., Mouchane, M., Taybi, H., Mouadili, A. (2025). Comprehensive Review on the Adsorption Properties of Clay Minerals for Enhanced Removal of Toxic Dyes and Heavy Metals, *Journal of Water and Environmental Nanotechnology*, *10*(1), 85-107. doi: https://doi.org/10.22090/jwent.2025.01.08

Li, H. (2024). Dynamic Modeling and Simulation of SAG Mill Circuits with Pebble Crushing, *Chalmers Tekniska Hogskola* (Sweden). doi: 10.1016/j.mineng.2018.07.010

Li, Y., Bao, J., Chen, T., Yu, A., Yang, R. (2022). Prediction of ball milling performance by a convolutional neural network model and transfer learning, *Powder Technology*, *403*, 117409. doi: 10.1016/j.powtec.2022.117409

Lowrison, G.C. (1974). Crushing and Grinding, The size Reduction of Solid Materials, CRC Press Inc.

Makgoale, D.M. (2019). Effects of mill rotational speed on the batch grinding kinetics of a UG2 platinum ore, Master Thesis, Engineering: Chemical, University of South Africa, South Africa.

Maleki-Moghaddam, M., Yahyaei, M., Banisi, S. (2013). A method to predict shape and trajectory of charge in industrial mills, *Minerals Engineering*, *46*, 157-166. doi: 10.1016/j.mineng.2013.04.013

Matsanga, N., Nheta, W., Chimwani, N. (2023). A review of the grinding media in ball mills for mineral processing, *Minerals*, *13*(11), 1373. https://doi.org/10.3390/min13111373

Mori, H., Mio, H., Kano, J., Saito, F. (2004). Ball mill simulation in wet grinding using a tumbling mill and its correlation to grinding rate, *Powder Technology*, *143*, 230-239. doi: 10.1016/j.powtec.2004.04.029

Morrell, S. (1993). The prediction of power draw in wet tumbling mills. PhD thesis, Department of Mining and Metallurgical Engineering, University of Queensland. doi: 10.13140/RG.2.1.3189.2248

Morrell, S. (1996). Transactions of the Institution of Mining and Metallurgy, 105.

Morrell, S. (2004). A new autogenous and semi-autogenous mill modeling for scale-up, design and optimization, *Minerals Engineering*, *17*, 437-445. doi: 10.1016/j.mineng.2003.10.013

Morrell, S. (2009). Predicting the overall specific energy requirement of crushing, high pressure grinding roll and tumbling mill circuits, *Minerals Engineering*, *22*, 544-549. doi: 10.1016/j.mineng.2009.02.007

Morrell, S. (2016). Modeling the influence on power draw of the slurry phase in Autogenous (AG), Semi-autogenous (SAG) and ball mills, *Minerals Engineering*, *89*, 148- 156. doi: 10.1016/j.mineng.2016.01.015

Morrell, S. (2019a). SME Mineral Processing & Extractive Metallurgy Handbook, Englewood: *Society for Mining, Metallurgy & Exploration*.

Morrell, S. (2019b). Modelling Approaches and Their Application in Comminution Circuit Design, SMC Testing, September, http://www.smctesting.com.

Morrison, R.D., Morrel, S.L. (1997). Comminution Practices (No. CONF-970211-), *Society for Mining, Metallurgy and Exploration*, Inc., Littleton, CO (United States), R.K. Kawatra (ed), SME, Colorado, 139-146.

Mular, A.L., Halbe, D.N., Barratt, D., J. (2002). Mineral Processing Plant Design, Practice, and Control, *1*, Published by SME.

Ngcobo, S., Silwana, B., Maqhashu, K., Matoetoe, M. C. (2022). Bentonite nanoclay optoelectrochemical property improvement through bimetallic silver and gold nanoparticles, *Journal of Nanotechnology*, *2022*(1), 3693938. doi: 10.1155/2022/3693938

Prasher, C.L., (1987). Crushing and Grinding Process Handbook, John Wiley & Sons Ltd. https://doi.org/10.1002/cite.330610129

Rockson-Itiveh, D. E., Keke, M., Ozioko, F. C., Otuya, I. C. (2023). Bentonite Clay as an Alternative Adsorbent for Removal of Heavy Metals in Wastewater, *FUOYE Journal of Engineering and Technology*, *8*(3). doi:10.46792/fuoyejet.v8i3.1033

Shields, L., Silva, J., Calnan, J., Maldonado, E., Agioutantis, Z. (2024). Integrating Underground Blast Fragmentation Modeling for Sustainable Mine-to-Mill Optimization: A Focus on Blast Fragmentation and Energy Efficiency in Comminution Circuits, *Rock Mechanics and Rock Engineering*, 1-12. doi: 10.1007/s00603-024-03755-2

Stojiljković, S. T., Stojiljković, M. S. (2017). Application of bentonite clay for human use, *Proceedings of the IV Advanced Ceramics and Applications Conference* (pp. 349-356), Atlantis Press. doi: 10.2991/978-94-6239-213-7_24

Upadhyay, R. K. (2025). Mining, Mineral Beneficiation, and Environment, In Geology and Mineral Resources, 799-858, Singapore: Springer Nature Singapore. doi: 10.1007/978-981-96-0598-9_12

Vetyugov, D., Matveeva, T. (2024). Research for Industrial Application of Bentonite-Polymer Material, *Recent Advances in Montmorillonite*, *87*. doi: 10.5772/intechopen.1005393

Wan, A., Du, C., Chen, T., He, J., Al-Bukhaiti, K. (2024). Intelligent process control system for predicting operating conditions of slag grinding machines: a data mining approach for improved efficiency and energy savings, *Mineral Processing and Extractive Metallurgy*, *133*(1-2), 7-20. doi: 10.1177/08827508231225018

Wang, H., Ito, D., Shirakawabe, T., Ruan, K., Komine, H. (2024). On swelling behaviours of a bentonite under different water contents. *Géotechnique*, *74*(1), 64-80. doi: 10.1680/jgeot.21.00312

Wikedzi, A. (2020). Assessment of the performance of grinding circuit for Buzwagi Gold Mine, *Tanzania Journal of Engineering and Technology*, *39*(2), 144-164. doi: 10.52339/tjet.v39i2.702

Wills, B.A. (1997). Mineral Processing Technology, 6th Edition, Butterworth Heinemann.

Yıldırım, Ö., Arıol, H., Sabah, E. (2025). Multi objective optimization of dry batch micronized grinding of slaked lime in a vibrating mill via TOPSIS and ANOVA, *Separation Science and Technology*, 1-14. doi: 10.1080/01496395.2025.2458620

Zhang, H., Du, S., Wang, Y., Xue, F. (2024). Prevention of Crystal Agglomeration: Mechanisms, Factors, and Impact of Additives, *Crystals*, *14*(8), 676. doi: 10.3390/cryst14080676

SAŽETAK

Inovativni pristup optimizaciji kruga mljevenja u postrojenju za proizvodnju mikroniziranoga praha

Istraživanje je provedeno s ciljem analize i optimizacije kruga mljevenja u proizvodnome postrojenju tvrtke Arak, specijaliziranome za proizvodnju mikroniziranoga bentonitnog praha. Kriteriji vrednovanja obuhvaćali su optimalne performanse sustava mljevenja, energetsku učinkovitost opreme te istodobnu optimizaciju ulazne i izlazne granulacije, kapaciteta i specifične potrošnje energije. Uz Bondovu formulu u analizi su kao inovativan pristup primijenjene i Morrellove te Austinove jednadžbe s naglaskom na utjecaj radnih parametara poput brzine vrtnje i stupnja ispunjenosti mlina. Glavna operacija usitnjavanja u predmetnome postrojenju odvija se u cilindričnome mlinu s kuglama, koji je konfiguriran u zatvorenome krugu s dvama zračnim separatorima. Konačni proizvod dostiže finoću manju od 75 μm, uz specifičnu potrošnju energije od 48 kWh po toni bentonita. Analiza je pokazala da se približno 59 % ukupne potrošnje energije postrojenja odnosi na krug mljevenja mlina s kuglama. Ulazna veličina čestica (d_{80}) iznosila je 3500 μm, stupanj popunjenosti i akumulacije materijala bili su 21 % i 14 %, prosječni promjer kugli iznosio je 60 mm, a relativna brzina vrtnje mlina 79 %. Rezultati su uputili na nisku učinkovitost kruga mljevenja, tek oko 30 %. Provedene simulacije i prijedlozi optimizacije pokazuju da bi se povećanjem stupnja popunjenosti mlina s kuglama od 21 % na 70 %, povećanjem ulazne granulacije na 7000 μm, uporabom kugli promjera manjega od 40 mm te smanjenjem relativne brzine vrtnje na 60 % mogla ostvariti povećana učinkovitost kruga mljevenja i do 50 %. Dodatno je utvrđeno kako se približno 16 % krupnih čestica u proizvodu javlja u obliku aglomerata, pri čemu njihovo smanjenje ima izravan utjecaj na smanjenje specifične potrošnje energije i povećanje ukupne učinkovitosti procesa mljevenja.

Ključne riječi:
mikronizirani prah, energetska učinkovitost, cilindrični mlin s kuglama, bentonit, Morrellove i Austinove jednadžbe

Author's contribution

Alireza Ghorbanifar (Master's degree, Department of Mining Engineering, Islamic Azad University) gathered samples, characterized the samples, and contributed to the crushing, grinding and separation processes and described the characterization and evaluation of the final products. **Marzieh Hosseini Nasab** (Associate Professor, Faculty of Mining Engineering, University of Sistan and Baluchestan) also contributed to the crushing, grinding and separation processes. Supervision, validation, visualization, writing – original draft and writing – review & editing were her other responsibilities for this research. **Javad Alibabaii** (Master's degree, School of Mining Engineering Tehran) and **Mohammad Noaparast** (Professor of Mineral Processing, Faculty of Mining Engineering, Department of mineral processing, University of Tehran) evaluated the results, reviewed the draft manuscript, and provided technical suggestions.
All authors have read and agreed to the published version of the manuscript.